CloudSat Project
A NASA Earth System Science Pathfinder Mission

Level 2 GEOPROF Product Process Description and Interface Control Document

Version: 3.0
Date: July 30, 2004

Questions concerning the document and proposed changes shall be addressed to

Gerald Mace
mace@met.utah.edu
(801) 585-9489

Cooperative Institute for Research in the Atmosphere
Colorado State University
Fort Collins, CO 80523

Contents

1. Introduction

The presence or absence and vertical location of cloud layers impose powerful constraints on the radiative properties of an atmospheric column and, thereby, modulate strongly the radiative heating rate of the column. Comprehensive information on the vertical distribution of cloud layers have been largely missing from analyses of conventional passive-sensor satellite radiometers that observe only the emitted and reflected radiance from the atmosphere and surface. Conventional satellite data have only allowed us to crudely estimate the location and vertical extent of clouds. Active remote sensors such as CloudSat, on the other hand, are uniquely adapted to observe the vertical location of hydrometeor layers. Therefore, a basic requirement of the CloudSat project is to use data from the Cloud Profiling Radar (CPR) to identify those levels in the vertical column sampled by CloudSat that contain significant radar echo from hydrometeors and to produce an estimate of the radar reflectivity factor for each volume deemed to contain significant echo (Stephens et al, 2001).

The CloudSat orbit will follow closely the orbit of the EOS PM1 satellite (Aqua) on which a number of advanced passive remote sensors will observe the earth. This synergistic association can add significantly to our understanding of the CloudSat geometrical profile and we will use this data source to our advantage. In particular, the Moderate-Resolution Imaging Spectroradiometer (MODIS) will provide information regarding the occurrence and horizontal distribution of clouds within the CloudSat footprint. The MODIS cloudmask product (Ackerman et al., 1998) will be available for use in the operational CloudSat processing stream. The MODIS cloudmask contains not only an estimate of the likelihood of clouds in 1km MODIS pixels, but also contains the results of a number tests with MODIS-observed spectral radiances that will provide limited information on the nature of the clouds in the vertical column. We will use the results of these tests to help us evaluate the characteristics of the CPR hydrometeor returns by performing comparisons of the CPR hydrometeor mask and the MODIS spectral tests.

This document describes the algorithm that will be implemented operationally to identify significant radar echo in the CloudSat data stream. The goals of the algorithm are to

- Examine the characteristics of each range resolution volume to determine if the radar data for that volume is significantly different from the radar noise characteristics and, thus, deemed to contain hydrometeors,
- Quantify the likelihood that a given range resolution volume with characteristics different from noise actually contains hydrometeors,
- Compare the radar significant echo profile with the information from the MODIS cloud mask.

2. Algorithm Theoretical Basis

The Geometrical Profile (GEOPRO) algorithm will contain two parts. The first part will be designed to identify significant radar echo in profiles of returned radar power in the CloudSat CPR data. The second part will consist of a comparison of the geometrical profile algorithm with the MODIS cloud mask spectral tests. This comparison will allow for an initial comparison of the CloudSat profile and the MODIS cloud mask.

2.1 The Significant Echo Mask Algorithm

The CPR records range-resolved profiles of backscattered power. These measurements as contained in the level 1B input data represent a 0.16 s average of returned power that correspond nominally to a horizontal resolution of 2.5 km along track by 1.2 km across track. The range resolution is 500 m and will be oversampled to generate a range gate spacing of 250m.

The goal of the significant echo mask (SEM) portion of the GeoProf algorithm is to identify those resolution volumes that contain signal that is significantly different from noise and establish the likelihood that such volumes contain hydrometeors. The goal of the SEM algorithm is to maximize the identification of hydrometeor echo while minimizing the occurrence of false alarms (false alarms are defined as range resolution volumes identified as contain hydrometeor return when none actually exits). Since the CPR minimum detectable signal is –28 dBZ_e, some hydrometeor layers will have a backscatter crosssection per unit volume that generates signal near or below the detection threshold of the CPR. It is necessary, therefore, to carefully tune the SEM to extract all possible significant signals from the radar returns. In formulating the SEM, we will generally follow the approach outlined by Clothiaux et al (1995 and 2000) with some modifications as described below. The level 1b data that will be available to the GEOGROF algorithm will include the power return $P_{r,jk}$ in each resolution volume where subscript j defines the along track dimension and k the vertical dimension. Given the pulse repetition frequency of 4300 Hz, and the averaging time of 0.16s, $P_{r,jk}$, represents an average of nominally 688 pulses. The measured value is composed of a sum of power return from the atmosphere ($P_{h,jk}$) and a Gaussian-like background system noise power ($P_{n,jk}$) assumed to be due primarily to the mixer noise. Our initial criteria for a significant return is that $P_{r,jk} > P_{n,jk}+(3\sigma_n)$ where σ_n is the standard deviation of $P_{n,jk}$ estimated by examining P_n in nearby regions above the tropopause where we are certain no atmospheric return will be recorded in the reported values $P_{r,jk}$. If the noise characterization is accurate and Gaussian, approximately 0.25% of noise returns will be incorrectly labeled as significant echo, P_{sig}. While we can be certain that while there will be few occurrences where noise will be identified as significant, there will be hydrometeor returns where $P_{h,jk} < P_{n,jk}+(3\sigma_n)$. One of the major goals of the GEOPROF algorithm is to accurately identify these volumes.

In an effort to identify the relatively weak but significant radar returns, we will implement a statistical approach that effectively increases the separation between signal

and noise by assuming some degree spatial and vertical continuity of the hydrometeor field on the scales of the CloudSat observations. Consider a two-dimensional data window *m* resolution volumes along track and *n* resolution volumes in depth centered on some pixel whose power value is $P_{r,jk}<P_{n,jk}+(3\sigma_n)$. We can ascertain the likelihood of this resolution volume not containing significant radar echo by comparing the statistics of that pixel and its neighbors to the estimate of the noise statistics acquired from pixels known to not contain significant echo. The Gaussian probability that the pixel is noise

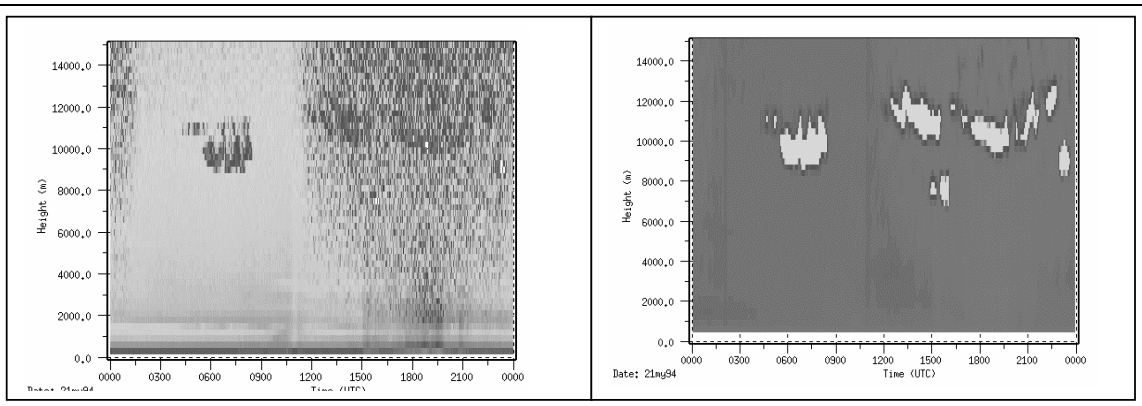

Figure 1. Example of the significant echo mask (SEM) algorithm applied to micropulse lidar data. In (a), the raw data shows evident cirrus during the night (low noise) and careful inspections shows that the layer persists into the day as the solar noise causes the background signal to increase. The SEM uses the statistics of these profiles to effectively increase the separation between signal and noise. In (b) the quantity p_{eff} is plotted. The light gray areas show p_{eff}<-30., the dark gray areas show –30.<p_{eff}<-20., and the medium gray areas show p_{eff}>-20.

can be expressed $p_i = \frac{1}{\sigma_n \sqrt{2\pi}} exp\left(-\frac{1}{2\sigma_n^2} \left(\overline{P}_r - P_{n,jk} \right)^2 \right)$ where $\overline{P}_r$ is the mean signal in the data window. Since a low value of *p* could arise due to significant signal anywhere in the data window, we assign *p* to all the resolution volumes in the data window. A value p_i is then calculated at each resolution volume for the data windows associated with it and the effective value of *p* (p_{eff}) for that volume is taken as $p_{eff} = \sum_i log(p_i)$ for the $i = m \times n$ times it has been examined in conjunction with its nearest neighbors. In the case of a weakly reflective but spatially persistent hydrometeor layer p_{eff} becomes substantially negative for the affected range gates. Figure1 demonstrates an example of this algorithm applied to lidar data. We present this particular example to highlight the ability of the statistical approach to effectively separate the signal from the noise. In figure 1 we see that the cirrus observed during the night (06-09 UTC) could be easily identified with a thresholding algorithm while cirrus observed during the day are much more difficult to identify because their backscattered signal is very close to the noise threshold. The statistical algorithm identifies those portions near 10 km that are temporally persistent and even identifies areas of cloudiness near 7 km that are not immediately obvious by a cursory visual inspection. In figure 1b, the lighter colored regions of the cloud layer are those portions where p_{eff} < -30. The darker gray areas surrounding the light shaded regions are somewhat ambiguous areas where p_{eff} < -20.

48 BIT CLOUD MASK FILE SPECIFICATION		
BIT FIELD	**DESCRIPTION KEY**	**RESULT**
0	Cloud Mask Flag	0 = not determined 1 = determined
1-2	Unobstructed FOV Quality Flag	00 = cloudy 01 = uncertain clear 10 = probably clear 11 = confident clear
PROCESSING PATH FLAGS		
3	Day / Night Flag	0 = Night / 1 = Day
4	Sun glint Flag	0 = Yes / 1 = No
5	Snow / Ice Background Flag	0 = Yes/ 1 = No
6-7	Land / Water Flag	00 = Water 01 = Coastal 10 = Desert 11 = Land
ADDITIONAL INFORMATION		
8	Non-cloud obstruction Flag (heavy aerosol)	0 = Yes / 1 = No
9	Thin Cirrus Detected (near infrared)	0 = Yes / 1 = No
10	Shadow Found	0 = Yes / 1 = No
11	Thin Cirrus Detected (infrared)	0 = Yes / 1 = No
12	Spare (Cloud adjacency)	(post launch)
1-km CLOUD FLAGS		
13	Cloud Flag - simple IR Threshold Test	0 = Yes / 1 = No
14	High Cloud Flag - CO_2 Threshold Test	0 = Yes / 1 = No
15	High Cloud Flag - 6.7 μm Test	0 = Yes / 1 = No
16	High Cloud Flag - 1.38 μm Test	0 = Yes / 1 = No
17	High Cloud Flag - 3.9-12 μm Test	0 = Yes / 1 = No
18	Cloud Flag - IR Temperature Difference	0 = Yes / 1 = No
19	Cloud Flag - 3.9-11 μm Test	0 = Yes / 1 = No
20	Cloud Flag - Visible Reflectance Test	0 = Yes / 1 = No
21	Cloud Flag - Visible Ratio Test	0 = Yes / 1 = No
22	Cloud Flag - Near IR Reflectance Test	0 = Yes / 1 = No
23	Cloud Flag - 3.7-3.9 μm Test	0 = Yes / 1 = No
ADDITIONAL TESTS		
24	Cloud Flag - Temporal Consistency	0 = Yes / 1 = No
25	Cloud Flag - Spatial Variability	0 = Yes / 1 = No
26-31	Spares	
250-m CLOUD FLAG - VISIBLE TESTS		
32	Element(1,1)	0 = Yes / 1 = No
33	Element(1,2)	0 = Yes / 1 = No
34	Element(1,3)	0 = Yes / 1 = No
35	Element(1,4)	0 = Yes / 1 = No
36	Element(2,1)	0 = Yes / 1 = No
37	Element(2,2)	0 = Yes / 1 = No
38	Element(2,3)	0 = Yes / 1 = No
39	Element(2,4)	0 = Yes / 1 = No
40	Element(3,1)	0 = Yes / 1 = No
41	Element(3,2)	0 = Yes / 1 = No
42	Element(3,3)	0 = Yes / 1 = No
43	Element(3,4)	0 = Yes / 1 = No
44	Element(4,1)	0 = Yes / 1 = No
45	Element(4,2)	0 = Yes / 1 = No
46	Element(4,3)	0 = Yes / 1 = No
47	Element(4,4)	0 = Yes / 1 = No

Table 1. Bitwise description of the elements of the MODIS cloud mask. (adapted from Ackerman et al., 1998)

The threshold value p_{thresh} needs to be carefully tuned to maximize the correct identification of weakly reflective returns while minimizing the occurrence of false alarms. Like most thresholds values there is some amount of arbitrariness associated with p_{thresh}. We are continuing working with the CloudSat test data set to attempt to establish values for p_{thresh}, and we will continue that work during the initial post launch phase of the mission. Our current approach is based on examining many years of cloud

cloud-masked MMCR data from all the DOE ARM sites. The MMCR unmasked returned power is averaged vertically and temporally to simulate the CloudSat resolution and noise is added to decrease the sensitivity of the MMCR and simulate the mixer noise estimated for the CPR. The SEM algorithm is implemented on the simulated CloudSat data and the value of p_{eff} at each range gate is compared to the full resolution cloud masked MMCR data. The fraction of times that a CloudSat resolution volume with a particular value of p_{eff} contains hydrometeors as observed by the cloud-masked MMCR data is defined as $Q_h(p_{eff})$. The quantity $Q_h(p_{eff})$ is then used as an objective measure of the likelihood that a particular value of p_{eff} if used as p_{thresh} will correctly identify the occurrence of hydrometeor in the layer. A value of 1- $Q_h(p_{eff})$ identifies the likelihood of that value of p_{eff} if used as p_{thresh} resulting in false alarms.

2.2 SEM-MODIS Mask Intercomparison

CloudSat is expected to orbit within several degrees and approximately 5 seconds behind the EOS PM (Aqua) satellite ground track. Aqua hosts a number of platforms that will add substantially to the information content of the CPR profile. The majority of this synergistic association between the CPR data and the Aqua data streams will be explored in a research mode during and after the flight phase of the CloudSat project. However, data from one these instruments (MODIS) will be acquired and ingested into the operational CloudSat processing stream. We will incorporate the MODIS cloud mask product (MOD35; Ackerman et al, 1998) as a quality/confidence check of the CloudSat GeoProf output.

MODIS cloudmask data will be available at the native 1 km (day and night) and 250m (daytime only) horizontal resolutions in an across track swath along the CloudSat ground track. Each data point is provided in the form of a 48 bit word (Table 1) for each 1km MODIS pixel. Details of this product can be found in Ackerman et al. (1998) and Ackerman et al. (1997). Table 1 provides a description of the information contained in the bitwise elements of the 48 bit word. Given the nominal CloudSat footprint of 1.4 km across by 2.5 km along track, several MODIS 1 km pixels can be examined to determine the likelihood that the CloudSat footprint is only partially filled with hydrometeors. This determination will be important to establishing the validity of the radar reflectivity factor reported by the GeoProf algorithm and will provide information that is critical to various level 2 processing algorithms that will attempt to determine the microphysical and radiative properties of hydrometeor layers. These algorithms often rely on an assumption that the backscatter cross section per unit volume is due to a reasonably uniform distribution of hydrometeors within that volume.

We must first determine if the hydrometeor vertical characteristics identified by the SEM and the hydrometeor field observed by MODIS are reasonably similar. It is understood that some fraction of the hydrometeor-filled resolution volumes sampled by CloudSat will have a reflectivity below the minimum detectable signal of the CPR and will go undetected. Studies suggest that these clouds will be composed of primarily near-tropopause cirrus and liquid phase mid-level and boundary layer clouds. Stephens et al (Stephens et al., 2001) show that this characteristic of the CloudSat data does not detract from the main mission of the project – namely to characterize the radiative heating of the atmospheric column. However, it will be helpful to identify which CPR columns appear to suggest significantly different cloud characteristics from that reported in the MODIS cloud mask product.

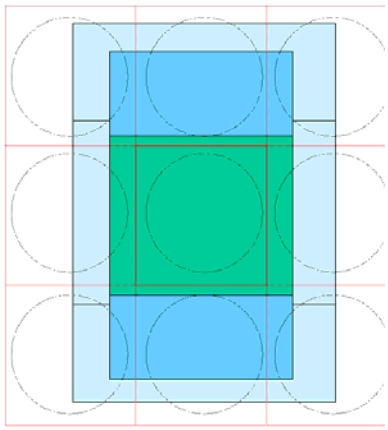

Figure 2. Schematic of the CloudSat-modis pixel configuration. The green rectangular area represents the 1.1 km region that will be most heavily weighted in the CloudSat CPR profile. The darker blue region will be less heavily weighted. The light green area represents the outer region that the CPR observational region due to pointing uncertainty. The grid square and circles represent the MODIS

The algorithm to compare the MODIS cloud mask and the CPR data will begin with a check of the status of the MODIS cloud mask and processing path used by the MODIS mask algorithm for the 15 1 km MODIS pixels nearest to the CPR profile in question. A weighting will be assigned to each pixel based on its location relative to the CloudSat footprint and the likelihood the pixel is within the CPR footprint. The schematic in Figure 2 illustrates the geometry of the problem accounting for the pointing uncertainty of the CPR of ~500 m. Once the pixel weighting is determined, bit 0 of each MODIS pixel will be examined to ensure that the MODIS mask has been implemented and the processing path for that pixel will be determined by examining bits 3-7 (see Table 1). The processing path bits identify which of the spectral tests are applicable. Bit 8 will also be examined to ensure that heavy aerosol (smoke or dust) was not present to significantly contaminate the visible channel radiances. By examining the spectral tests for each of the relevant MODIS pixels it will be possible to develop a broad characterization of the CloudSat scene. The level of detail that we can attain with this characterization will depend largely on the processing path taken by the MODIS cloudmask algorithm (Table 2). The processing path depends on the time of day and the surface ecosystem. The cloud characterization that we derive from the results of the cloud mask is limited to the following: 1) very thin high cloud, 2) thin high cloud, 3) thick high cloud, 4) high cloud, 5) mid level clouds, 6) low clouds, 7) non-high cloud. Table 3 shows which bits will be examined to determine a pixel characterization. In general, we will best be able to characterize the CloudSat scene in daytime over the unfrozen oceans because of the consistently dark and uniform background (when not in sunglint regions – bit 4). In general, scenes over nighttime land

		Day Ocean	Night Ocean	Day Land	Night Land	Polar Day (snow)	Polar Night (snow)	Coast Day	Coast Night	Desert Day	Desert Night
BT_{11}	(Bit 13)	✓	✓								
$BT_{13.9}$	(Bit 14)	✓	✓	✓	✓	✓	✓	✓	✓	✓	✓
$BT_{6.7}$	(Bit 15)	✓	✓	✓	✓	✓	✓	✓	✓	✓	✓
$R_{1.38}$	(Bit 16)	✓		✓		✓		✓		✓	
$BT_{3.7} - BT_{12}$	(Bit 17)				✓		✓				✓
BT_{8-11} & BT_{11-12}	(Bit 18)	✓	✓	✓	✓			✓	✓	✓	✓
$BT_{3.7} - BT_{11}$	(Bit 19)	✓	✓	✓	✓	✓	✓	✓	✓	✓	✓
$R_{.66}$ or $R_{.87}$	(Bit 20)	✓		✓				✓			
$R_{.87}/R_{0.66}$	(Bit 21)	✓		✓							
$R_{.935}/R_{.87}$	(Bit 22)	✓		✓		✓		✓			
$BT_{3.7} - BT_{3.9}$	(Bit 23)	✓		✓				✓		✓	
Temp Consis	(Bit 25)	✓	✓								✓
Spatial Variability	(Bit 25)	✓	✓								

Table 2. Modis cloudmask algorithm processing paths. The checks indicate which spectral tests are applied to a given ecosystem. Adapted from Ackerman et al., 1998.

will be difficult to characterize accurately due to the lack of a consistent IR background. Snow covered and other bright surfaces are also difficult to gauge accurately under many circumstances. These include desert, coastal, and mountainous regions.

High clouds are defined as having a cloud top pressure less than 500 mb and the designations of very thin, thin, and thick depend on the results of the spectral tests listed in Table 3. Taken together, these tests correspond in a broad sense to the optical thickness of the high layer. The thin and thick designations will be determined based on the results of IR and visible reflectance threshold tests reported in bits 13 and 20-22. For a high cloud to be classified as thick, we will require that it be thick enough to appear cold in the infrared window spectral region and be identifiable in at least one of the visible reflectance tests for daytime data. The most thorough test for thin and thick high clouds are possible over warm ocean surfaces due to the relative reliability of the IR threshold tests. Over daytime land the visible reflectance tests will be used. Along other processing paths it will not be possible to determine a thickness designation for high clouds using the MODIS cloud mask, thus the simple designation of high cloud will be used in the case that certain other bit tests suggest clouds above 500 mb. Bit 14, for instance, should be a reliable indicator of the presence of high clouds along any of the processing paths. The designation of very thin high clouds will be applied when the near IR spectral test (bit 9) suggests clouds but no other high cloud test is positive.

Thick mid level clouds will be discernable under some circumstances. Over the ocean, when bit 14 does not identify clouds then we can assume that the cloud top pressure is higher than 500 mb. However, if the cloud appears cold as reported by the IR threshold test (bit 13) and the underlying ocean is warm (as determined with meteorological data) we can reasonably suspect an optically thick cloud whose top is colder than freezing. During daytime, this classification will be aided by the use of visible reflectance tests since these cloud layers should be reflective in the visible and near infrared. Low-level clouds will be identified through various tests most of which are not implemented during the night. Thus we will often be unable to discriminate between clouds with tops in the middle and lower troposphere. These cases will be designated as non-high clouds.

Table 3. MODIS pixel cloudiness characterizations using cloudmask bit tests. Assumes the cloudmask has been implemented according to bit 0 and that the pixel has been classified as cloudy or low confidence clear by bits 1 and 2. The blacked out regions in this table denote cloud types in certain ecosystems that cannot be evaluated with confidence. More detailed flow charts are shown in Appendix A.

			Bits Examined for specific ecosystems							
Designation	Numerical Designation	MODIS Bit Value	Day Ocean	Night Ocean	Day Land	Night Land	Polar Day (snow)	Polar Night (snow)	Desert Day	Desert Night
Unclassifiable	9	Bit tests provide contradictory results for a cloudy pixel								
No Test	0	0	0							
Clear	1	10,11	1 and 2							
High Cloud	2	0	14	14	14	14	14	14	14	14
		1								
High Cloud, Very Thin	3	0	9	17	9	17	9	17	9	17
		1	13, 16	13	16	14	14	14	14	14
High Cloud, Thin	4	0	14, 16, 9	14, 11, 17	14, 16, 9					
		1	13, 22	13	22					
High Cloud, Thick	5	0	14, 16, 9, 13, 20, 21	14, 13	14, 16, 9, 20, 21					
		1								
Non High Cloud	6	0	13, 20, 21, 22, 19, 23	13, 18	20, 21, 22, 19, 23	18	22, 19		18, 23	18
		1	14, 9	14, 11	14, 9, 11, 16	14	14, 9		14, 9, 16	14, 11
Mid Cloud, Thick	7	0	13, 20, 21, 22, 19, 23	13						
		1	14, 9, 16	14, 16						
Low Cloud	8	0	20, 21, 22, 19, 23	18						
		1	13, 14, 9, 16	13, 14, 16						

Seemingly disparate possibilities will also be encountered and will be listed as unclassifiable. For instance, the thin cirrus identified by only the near IR threshold test (bit 9 or bit 16) will often be so thin that other tests will not be biased by its presence. Thus it will not be uncommon to encounter pixels that contain low-level clouds identifiable in the solar reflectance tests and thin cirrus. This situation is especially likely in the tropics and subtropics. Other possibilities include thin high clouds as observed by bit 14 with other low cloud indicators such as bits 19 or 18. These circumstances will often be indicative of multi-layered situations that can be verified in some circumstances with CloudSat data. Once the MODIS pixels composing a CloudSat footprint are characterized, the overall classification will be determined as a weighted mean of the various pixel types where thin and thick high cloud will be considered to compose a single type. To facilitate comparison between the CloudSat and Modis observations, the masked CPR data will be classified similarly according to Table 4.

Table 4. CPR echo top characterization

Cloud Classification	Numerical Designation	Definition
No Determination	0	
Clear Profile	1	No hydrometeor layers found in CPR profile
High Cloud	2	Echo top pressure less than 500 mb.
Mid Level cloud	3	Echo top pressure greater than 500 mb and echo top temperature colder than 273.
Low Level cloud	4	Echo top pressure greater than 500 mb and echo top temperature warmer than 273.
Multi Layer	5	Distinct combinations of above types

A variability classification will also be assigned to the scene using the 1km classified Modis pixels that compose the CloudSat footprint and immediately adjacent region (6-9 pixels) and will be labeled according to the criteria in Table 5.

Table 5. CloudSat Scene Variability Designation

CloudSat Scene Variability	Numerical Designation	Fraction of MODIS pixels in the vicinity of the CloudSat footprint with same cloud type
No Determination	0	
Highly Uniform	1	≥ 0.9
Uniform	2	≥ 0.75
Weakly Variable	3	$0.5 - 0.75$
Variable	4	≤ 0.5
Highly Variable	5	≤ 0.25

Additionally, during daylight regions over ocean (not including sun glint), bits 32-47 record the results of simple visible threshold tests applied to the central 16 250m pixels of a 1km MODIS pixel. Since only two channels are used to establish the presence of cloudiness in the 250m pixels, the uncertainty in each pixel is expected to be larger than the associated 1km value. However, our goal is to estimate the degree of scene uniformity. The overall cloud fraction provided by these tests will be useful for establishing this uniformity. This fractional cloud cover will, therefore, be calculated as a weighted mean of the MODIS pixels composing the field of view and recorded in tenths of coverage.

Our primary goal with this comparison is to establish the overall complimentarity of the combined data stream. In cases where we can establish that the CloudSat and MODIS representations are similar in regions with uniform cloudiness, then higher order algorithms can be implemented with confidence. In the opposite case, when the MODIS and CloudSat representations are different significantly, we will know that caution will need to be exercised in the application and interpretation of retrieval. Ultimately, this

comparison will improve our understanding of both data sets since much more detail will be available than either could provide alone.

2.3 Validation

Actual Comparison between CloudSat and MODIS data will obviously not be possible until after both instruments are generating data in orbit. We developed a library of cloud cases from several ground validation sites. These cases include Terra and Aqua MODIS scenes, millimeter radar and other ancillary data that allow us to closely simulate the data streams that will be available during the CloudSat mission. This library of cases covers a wide range of cloud types over multiple ecosystems. This library includes 313 real cases of millimeter radar data from three ARM sites and the corresponding MODIS data (Appendix C). It includes clear sky, high clouds (very thin, thin and thick high clouds), middle clouds, low clouds and multi-layer clouds.

3. Algorithm Inputs

3.1. CloudSat

3.1.1. CloudSat Level 1B CPR Science Data

The CPR Level 1 B (Li and Durden, 2001) is the main input for the GEOPROF Algorithm. 2B-GEOPROF algorithm requires the following inputs from the Level 1B CPR Science Data are (see Level 1B CPR Process Description and Interface Control Document). Spacecraft latitude and longitude are used to locate the position of satellite. Range bin sizes, Range to first bin, and Surface bin number are used to locate the height of resolution volumes. Received echo power is used as input to the SEM algorithm and for calculation of radar reflectivity. Radar transmission power, wavelength, and radar calibration coefficients are also needed when calculating radar reflectivity.

- Spacecraft latitude
- Spacecraft longitude
- Spacecraft altitude
- Range bin sizes
- Range to first bin
- Surface bin number
- Wave length
- CPR radar calibration coefficients
- Radar transmission power
- Received echo power

3.1.2. CloudSat Level 1A Auxiliary Data

Level 2 GEOPROF processing requires the following data:

- Land/Sea Flag
- Altitude of Surface

3.2. Ancillary (Non-CloudSat)

3.2.1. MODIS cloud mask data

The MODIS cloud mask data will be used for the comparison of the geometrical profile algorithm with the MODIS cloud mask spectral tests.

- MODIS latitude
- MODIS longitude
- 48 bit MODIS mask data in a swath along the CLOUDSAT ground track

3.2.2. ECMWF

Meteorological data interpolated temporally and spatially to the CLOUDSAT range resolution volumes are needed to aid in the comparison of MODIS mask data with CLOUDSAT profile data. Temperature and pressure profiles are required for the calculation of CPR echo top characterization (see Table 4).

- Temperature profile
- Atmosphere pressure profile

3.3. Control and Calibration

This algorithm does not require control and calibration data.

4. Algorithm Summary

4.1. The Significant Echo Mask Algorithm

The CPR records range-resolved profiles of backscattered power. The SEM algorithm is designed for identification of hydrometeor echo.

Read Level 1 B data granule
Put in loop over granule
Use Level 1 B Data

If $P_r \geq (P_n + (3\sigma_n))$ *then*
    cloud was detected
    set cloud_mask = 1;
end-if

while $P_r \leq (P_n + (3\sigma_n)))$ *then*
    consider spatial and vertical continuity
    calculate Gaussian probability that p_r *is noise in* 3×3 *box*
    calculate p_{eff} *--- the effective value of p*
        $p_{eff} = \Sigma(\log(p))$
    calculate quality assurance Q_A

    if $(p_{eff} \geq p_{thresh})$*then*
        cloud was detected
        cloud_mask = 1
    else
        no cloud
        cloud_mask = 0
    end-if
end-while

$P_r = P_r \times$ *cloud_mask*
calculate reflectivity

output radar reflectivity
output CPR cloud mask
output quality assurance Q_A (under development)

4.2 SEM-MODIS Mask Intercomparison

To summarize, the steps in Intercomparison of SEM and MODIS are:

Read MODIS cloud mask and MODIS navigation data
Read ECMWF data

Identify appropriate MODIS pixels
Determine pixel weighting to CLOUDSAT footprint

Determining MODIS cloud classification
If (bit 0 equals 0) then
No MODIS determination is needed
Else
If (bit 1, 2 equal 10 or bit 1, 2 equal 11) then
Clear atmosphere
Else
Determining MODIS cloud classification using the flow charts in Appendix A.
Check the surface ecosystems
Check the bits to determining cloud classification
End-if

Determining CPR cloud classification (Table 4)

Calculate CloudSat scene variability (Table 5)

Calculate cloud fraction with 250m pixels when possible

Output MODIS cloud classification
Output CPR echo top characterization
Output CloudSat scene variability
Output MODIS 250m cloud fraction

5. Data Product Output Format

5.1. Format Overview

The CPR Level 2 GEOPROF Product will produce an estimate of the radar reflectivity factor and cloud mask.

The format chosen for CPR Level 2 GEOPROF data is similar to that for CPR Level 1 B data. The format consists of metadata, which describes the data characteristics, and swath data, which includes the radar reflectivity factor, cloud mask and other information. The following schematic illustrates how GEOPROF data is formatted using HDF EOS. The variable nray is the number of radar profiles (frames, rays) in a granule. Each block is a 0.16 s average of radar data.

Table 6. CPR Level 2 GEOPROF HDF-EOS Data Structure

Data Granule	CloudSat Metadata			TBD
	CPR Metadata			TBD
	Swath Data	Time		Table: nray 10 bytes
		Geolocation		2 × nray 4-byte float
		SEM	Radar Reflectivity	125 × nray 2-byte integer
			Quality assurance Q_A	125 × nray 1 byte integer
			CPR Cloud Mask	125 × nray 1 byte integer
		SEM-MODIS	MODIS scene characterizations (Table 3)	nray, 1 byte
			CPR echo top characterizations (Table 4)	nray, 1 byte
			MODIS scene variability (Table 5)	nray, 1 byte
			MODIS 250m cloud fraction	nray, 1 byte

5.2. CPR Level 2 GEOPROF HDF-EOS Data Contents

The contents of the metadata are still TBD and so the sizes are also TBD.

- **CloudSat Metadata** (Attribute, Size TBD)

TBD by CIRA

- **CPR Metadata** (Attribute, Size TBD)

TBD by CIRA

- **Time** (Vdata data, array size nray, record size 10 byte):

Time is determined based on VTCW time. See Table 2 of Li and Durden (2001) for data format.

- **Geolocation** (SDS, array size 2 × nray, 4-byte float):

As documented in Li and Durden (2001), geolocation is defined as the Earth location of the center of the IFOV at the altitude of the Earth ellipsoid. The first dimension is latitude and longitude, in that order. The next dimension is ray number. Values are represented as floating point decimal degrees. Off earth is represented as less than or equal to -9999.9. Latitude is positive north, negative south. Longitude is positive east, negative west. A point on the 180th meridian is assigned to the western hemisphere.

- **SEM product**

  - **Radar Reflectivity** (SDS, array size 125 × nray, 2-byte integer)

Radar reflectivity factor Z_e is calculated with the echo power (P_r) and other input data as described in Level 1B CPR Process Description and Interface Control Document (Li and Durden, 2001).

  - **Quality assurance Q_A** (SDS, array size 125 × nray, 1-byte integer)

Quality assurance Q_A is the likelihood that a CloudSat resolution volume with a particular value of p_{eff} contains hydrometeors as compared to MMCR data.

  - **CPR Cloud Mask** (SDS, array size 125 × nray, 1-byte integer)

Each CPR resolution volume is assigned 1 bit mask value:

0 = No cloud detected
1 = Cloud detected

- **SEM-MODIS product**

  - **MODIS scene characterizations (SDS, 1-byte integer)**

This data includes MODIS pixel cloudiness characterizations using cloudmask bit tests. See Table 3 for a detailed specification.

  - **CPR echo top characterizations (SDS, 1-byte integer)**

See Table 4 for the detail specification.

- **MODIS scene variability (SDS, 1-byte integer)**

MODIS scene variability includes the variability classification assigned to the CloudSat scene using the 1 km classified MODIS pixels that compose the CloudSat footprint and immediately adjacent region. See Table 5 for detail specification.

- **MODIS 250m cloud fraction (SDS, 1-byte integer)**

MODIS 250 m cloud fraction includes cloud fraction calculated with MODIS 250m pixels.

6. Operator Instructions

The Level 2 GEOPROF product processing software is integrated into the CloudSat Operational and Research Environment (CORE). It is called using the standard CORE procedure for calling modules to operate on data files. The output is in the form of an HDF-EOS structure in memory, which can be saved by CORE and passed on to other Level 2 processing.

For quality assessment purposes, quick look images of the significant echo mask algorithm is created that show the results of the SEM algorithm and the unmasked echo powers before the significant echo mask is created (Appendix B1, Figure 3). The orbit is divided into four even sections in the images. The upper panel is CLOUDSAT return echo power before the SEM mask is applied. The middle panel is CLOUDSAT radar reflectivity after the SEM mask is applied. Coherent regions of return different from the background noise apparent on the upper panel should be visible in the middle panel as significant echo return. The lower panel is MODIS unobstructed FOV quality flag (bit 1 and 2). The red, green, blue and black lines represent, respectively, cloudy, uncertain clear, probably clear and confidently clear. The CloudSat track follows the middle of the plot. By comparing the middle and lower panels, we are able to compare the coincidence between the measurements of CLOUDSAT and MODIS.

Statistics of CloudSat profiles and MODIS cloud classifications are generated for quality control of the SEM-MODIS algorithm. An ASCII file is created to save these statistics for each orbit. The file is written under directory "C:\Data\Devel\2B-GEOPROF\Output\". Description and a sample of the diagnostic statistics ASCII output are given in Appendix B2. Plots for the ASCII output are also made for quality assessment purposes. Description and a sample of the plots are given in Appendix B3.

2B-GEOPROF Algorithm requires data from 1b-CPR, MODIS-AUX and ECMWF-AUX. Table 7 lists the input data, and their source, units, range. It also gives the missing data and what output data elements will be affected if the data is missing.

Table 7. 2B-GEOPROF algorithm input data, and their source, units, range, variable effected (* Please refer to corresponding algorithm ICD)

Input Data	Source	Units	Assumed Input Range	Missing Data Value	2B GEOPROF Variable Effected
Time	1B-CPR	second	0 to 6e+008	*	
Spacecraft Altitude	1B-CPR	km	600 to 800	*	Radar reflectivity, Qa, CPR cloud mask, CPR echo Top,
CPR Latitude	1B-CPR	degrees	-90 to 90	*	Radar reflectivity, Qa, CPR cloud mask, CPR echo Top,
CPR Longitude	1B-CPR	degrees	-180 to 180	*	Radar reflectivity, Qa, CPR cloud mask, CPR echo Top,
Ray Header Lambda	1B-CPR	m	0.0031879 to 0.0031879	*	Radar reflectivity, Qa, CPR cloud mask, CPR echo Top,
RayHeader RangeBinSize	1B-CPR	m	239.8 to 239.8	*	Radar reflectivity, Qa, CPR cloud mask, CPR echo Top,
Surface Bin Number	1B-CPR		75 to 125	*	Radar reflectivity, Qa, CPR cloud mask, CPR echo Top,
Range to first bin	1B-CPR	m	680000 to 740000	*	Radar reflectivity, Qa, CPR cloud mask, CPR echo Top,
Transmit powers	1B-CPR	W	1500 to 2000	*	Radar reflectivity Qa, CPR cloud mask, CPR echo Top,
Received echo power	1B-CPR	dBm	-130 to -40	*	Radar reflectivity, Qa, CPR cloud mask, CPR echo Top
Radar coefficient	1B-CPR	m^{-3}		*	Radar reflectivity, Qa, CPR cloud mask, CPR echo Top,
MODIS	MODIS-AUX	degrees	-90 to 90	*	MODIS Scene Var

latitude					
MODIS longitude	MODIS-AUX	degrees	-180 to 180	*	MODIS Scene Var
MODIS cloud mask	MODIS-AUX		0 or 1	*	MODIS scene char MODIS Scene var MODIS cloud fraction
Air pressure	ECMWF-AUX	Pa	0 to 12000	*	CPR echo Top
Air temperature	ECMWF-AUX	K	30 to 253	*	CPR echo Top

Table 8 lists the 2B-GEOPROF Algorithm output data, and their units and range. If any of the required input data for a given variable are either missing or outside the expected range (see previous table), then the output variable will be set to its missing value.

Table 8. 2B-GEOPROF algorithm output data, and their units, range, required inputdata

2B GEOPROF Output Data	**Units**	**Range of Output Data**	**Missing Data**	**Required Input Data**
Radar reflectivity	dBz	-40.00 to 50.00	-88.88	Spacecraft Altitude, RayHeader Lambda, RayHeader RangeBinSize, Surface Bin Number, Range to first bin, Transmit powers, Received echo power, Radar coefficient
Quality assurance		0-1	-9	Spacecraft Altitude, RayHeader Lambda, RayHeader RangeBinSize, Surface Bin Number, Range to first bin, Transmit powers, Received echo power, Radar coefficient
CPR cloud mask		0 or 1	-9	Spacecraft Altitude, RayHeader Lambda, RayHeader RangeBinSize, Surface Bin Number, Range to first bin, Transmit powers, Received echo power, Radar coefficient
MODIS scene characterizations		0 to 9	-9	MODIS cloud mask
CPR echo top		0 to 5	-9	Spacecraft Altitude, RayHeader Lambda,

				RayHeader RangeBinSize, Surface Bin Number, Range to first bin, Transmit powers, Received echo power, Radar coefficient, Air pressure, Air temperature
MODIS Scene variability		0 to 4	-9	MODIS latitude, MODIS longitude, MODIS cloud mask
MODIS cloud fraction		0 to 100	-99	MODIS cloud mask

7. References

Ackerman, S. A., K. I. Strabala, W. P. Menzel, R. A. Frey, C. C. Moeller, L. E. Gumley, 1998: Discriminating clear sky from clouds with MODIS. *J. Geophys. Res.,* **103,** 32141-32157.

Clothiaux, E.E., G. G. Mace, T. P. Ackerman, T. J. Kane, J. D. Spinhirne, V. S. Scott, 1998: An Automated Algorithm for Detection of Hydrometeor Returns in Micropulse Lidar Data. *J. Atmos. and Oceanic Technol.*, **15,** 1035-1042,

Li, L. and S. Durden, 2001: Level 1 B CPR Process Description and Interface Control Document. Jet Propulsion Laboratory.

Stephens, G. A., D. Vane, and many others, 2001: The CloudSat mission and the EOS constellation: A new dimension to space-based observations of clouds and precipitation. Submitted to *Bull. Amer. Meteoro. Soc.*

8. Acronym List

SEM – Significant Echo Mask
MODIS – Moderate-Resolution Imaging Spectroradiometer

Appendix A. Flowcharts of MODIS pixel cloudiness characterizations

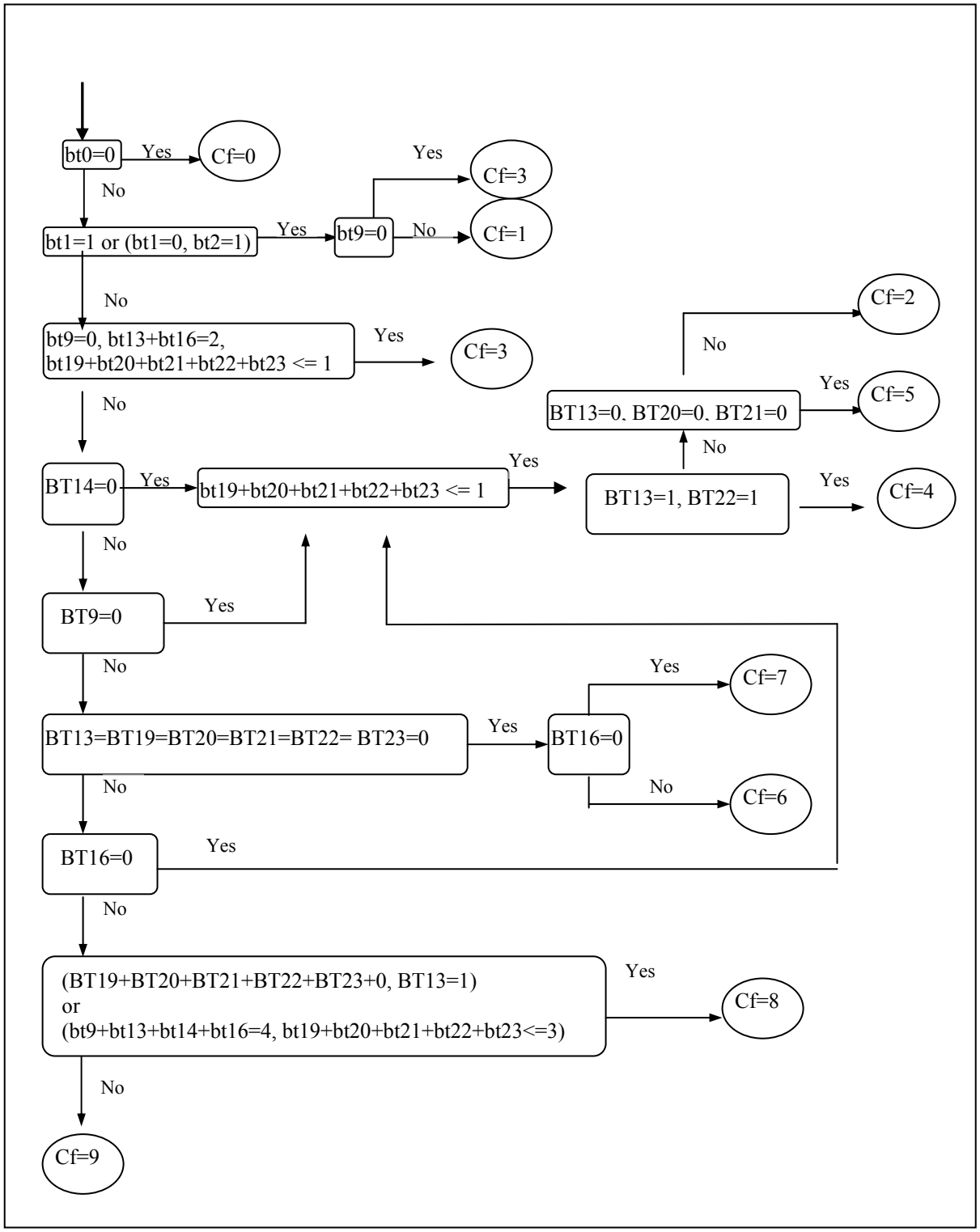

1. Flowchart of Ocean/Day

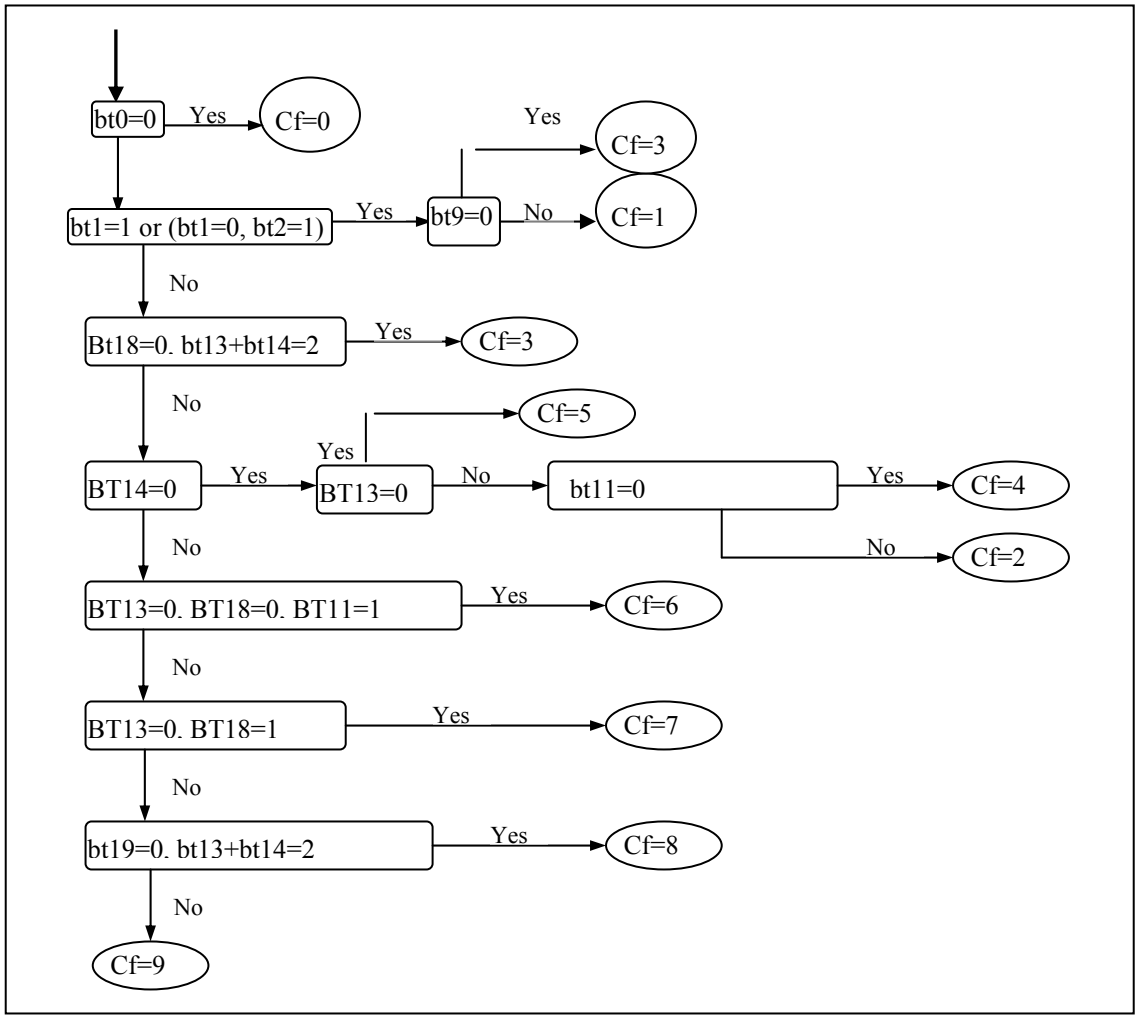

2. Flowchart of Ocean/Night

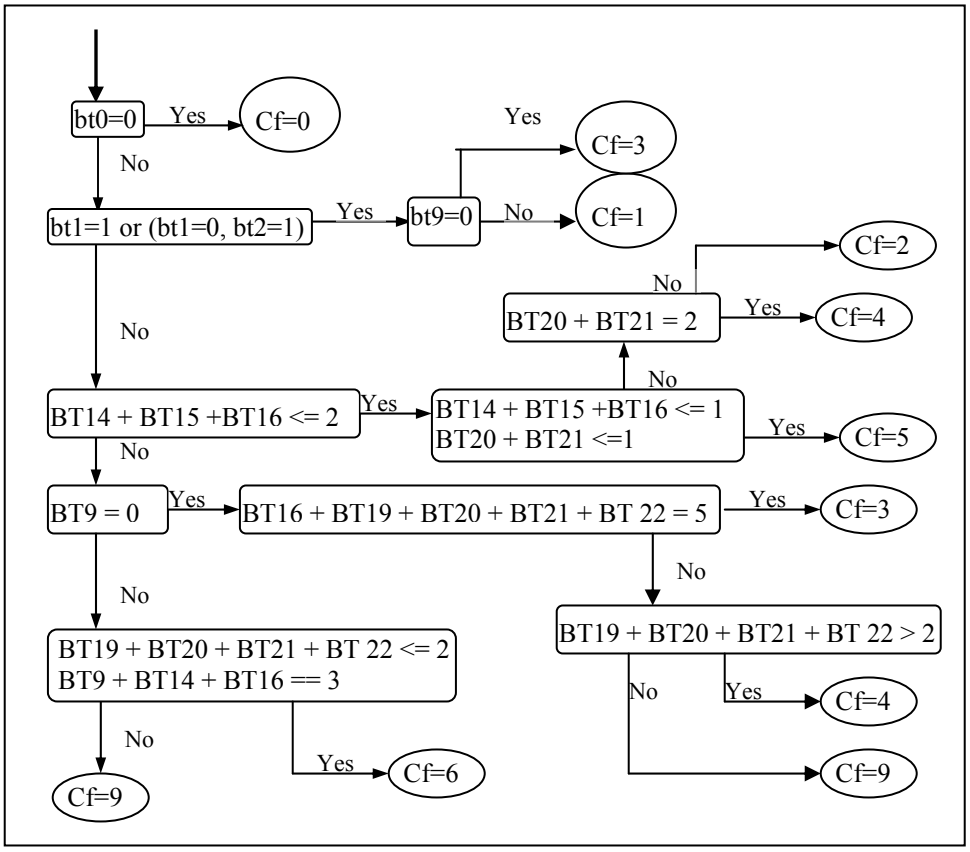

3. Flowchart of Land/Day

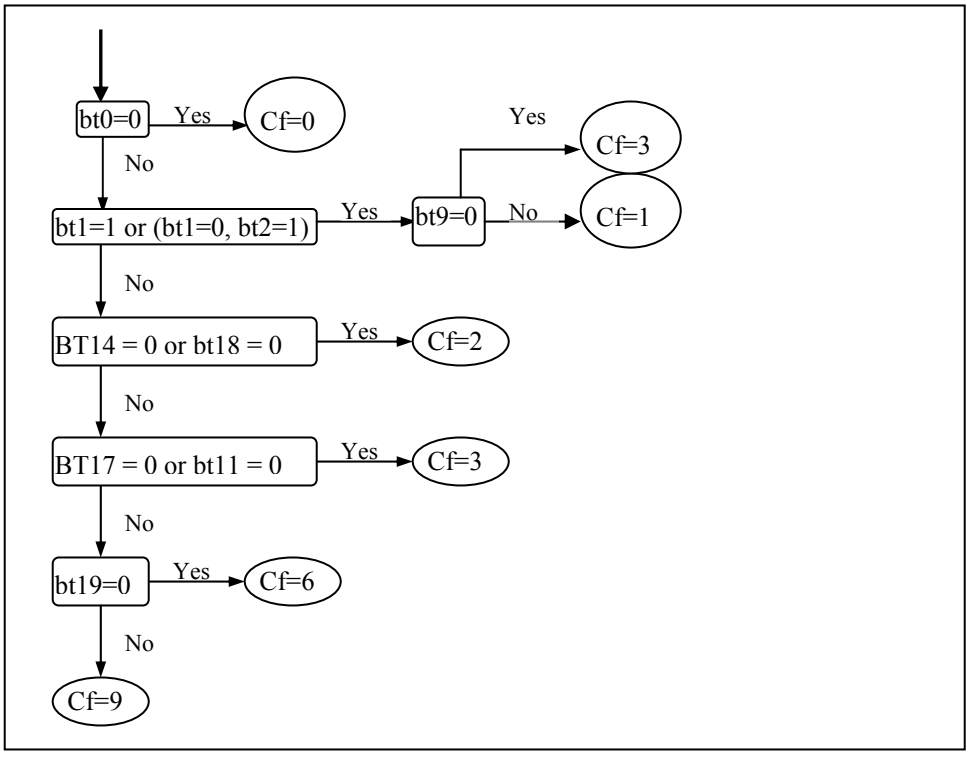

4. Flowchart of Land/Night

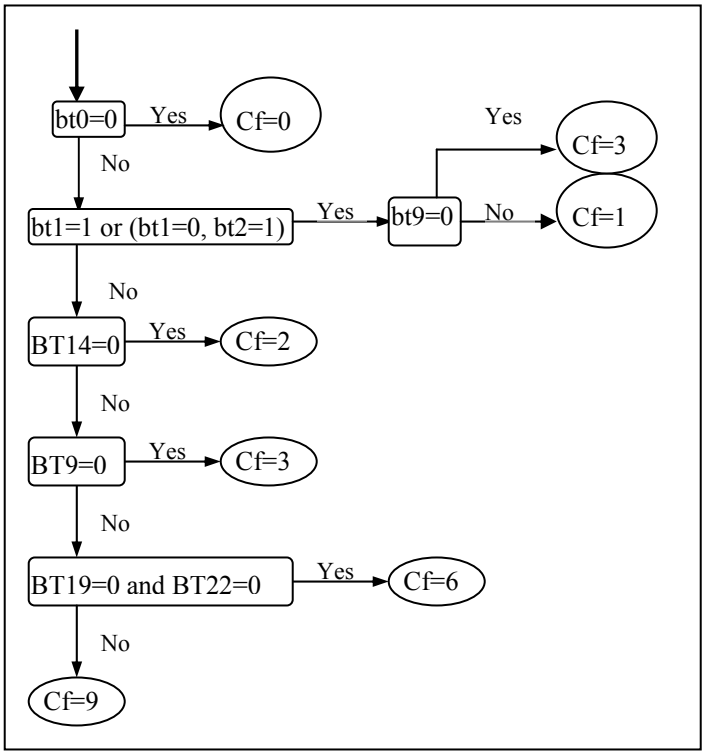

5. Flowchart of Polar/Day

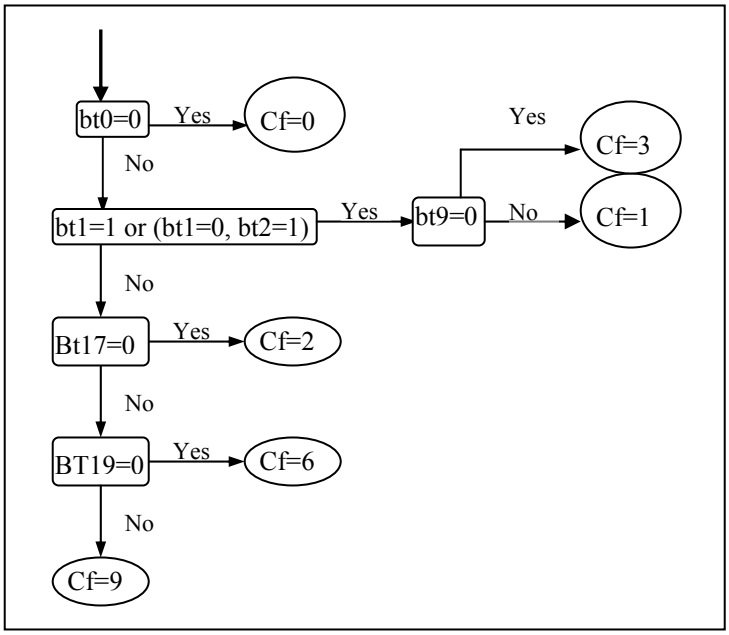

6. Flowchart of Polar/Night

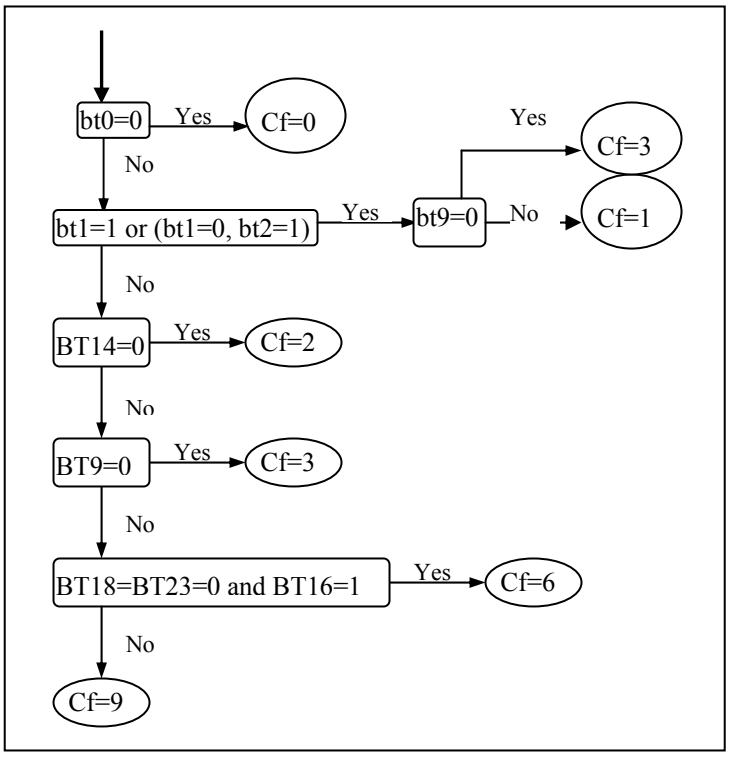

7. Flowchart of Desert/Day

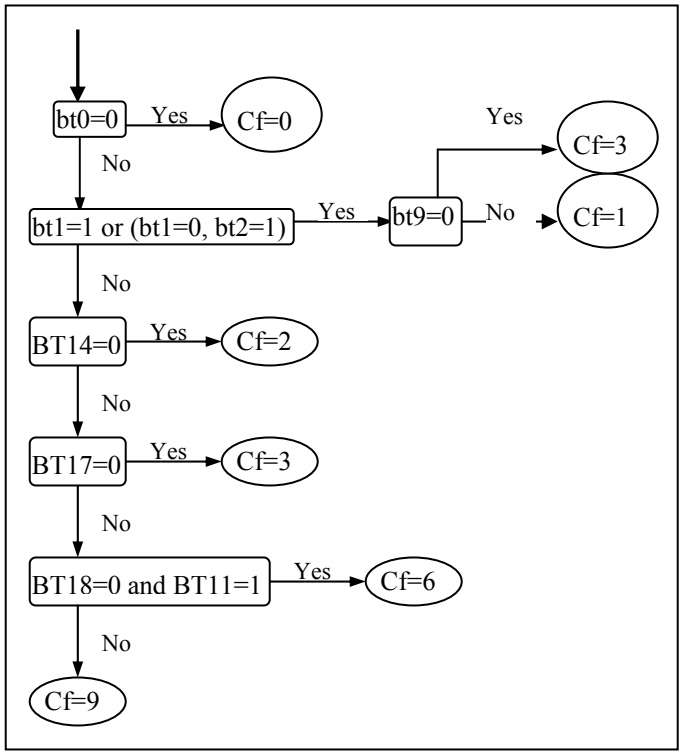

8. Flowchart of Desert/Night

Appendix B. Quality Assessment

B1. Plots of CLOUDSAT return echo power before the SEM mask, radar reflectivity after the SEM mask, and MODIS Unobstructed FOV Quality Flag for quality assessment purposes

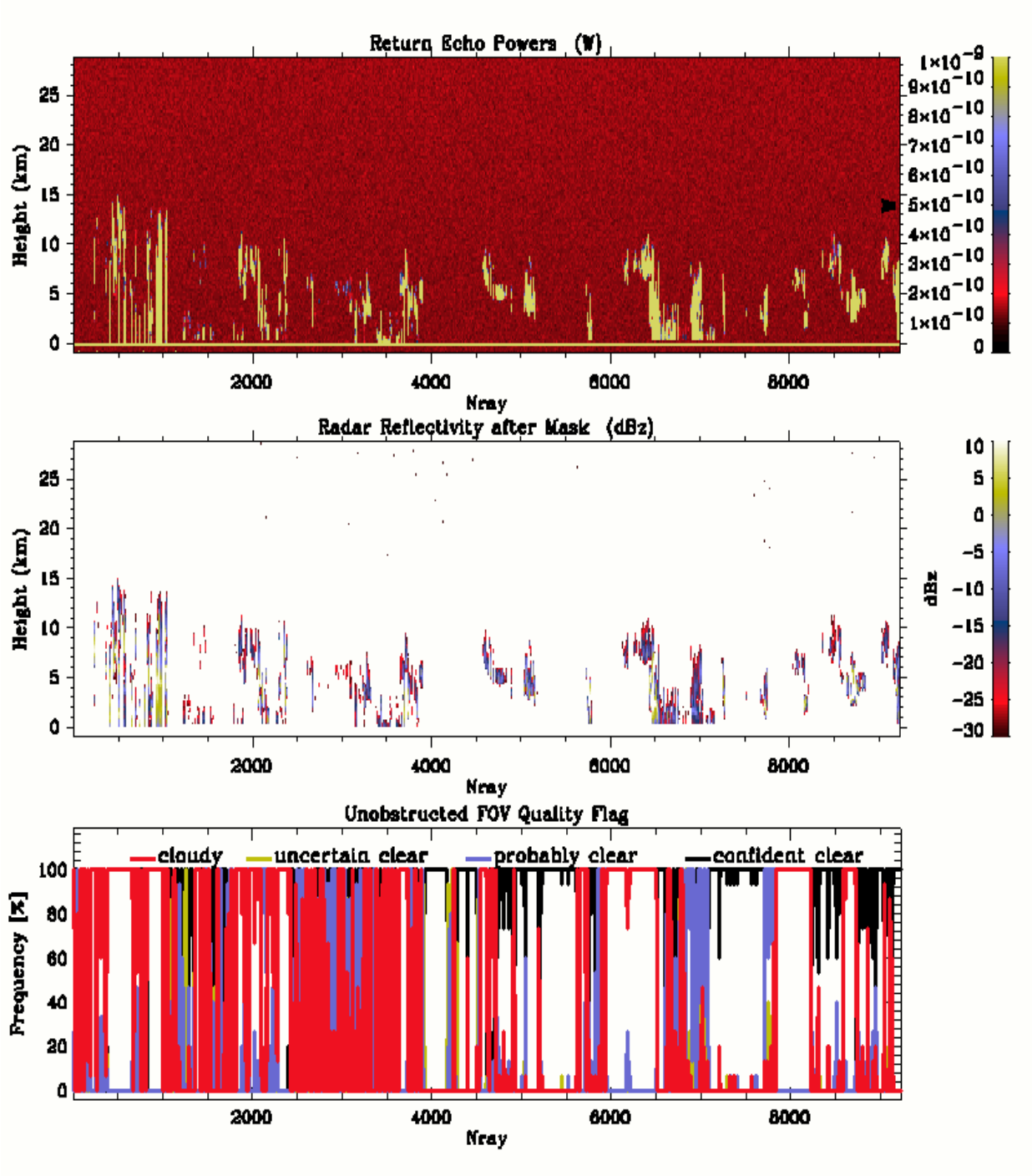

Figure 3(a). Return echo power before significant echo mask and radar reflectivity after mask (section 1).

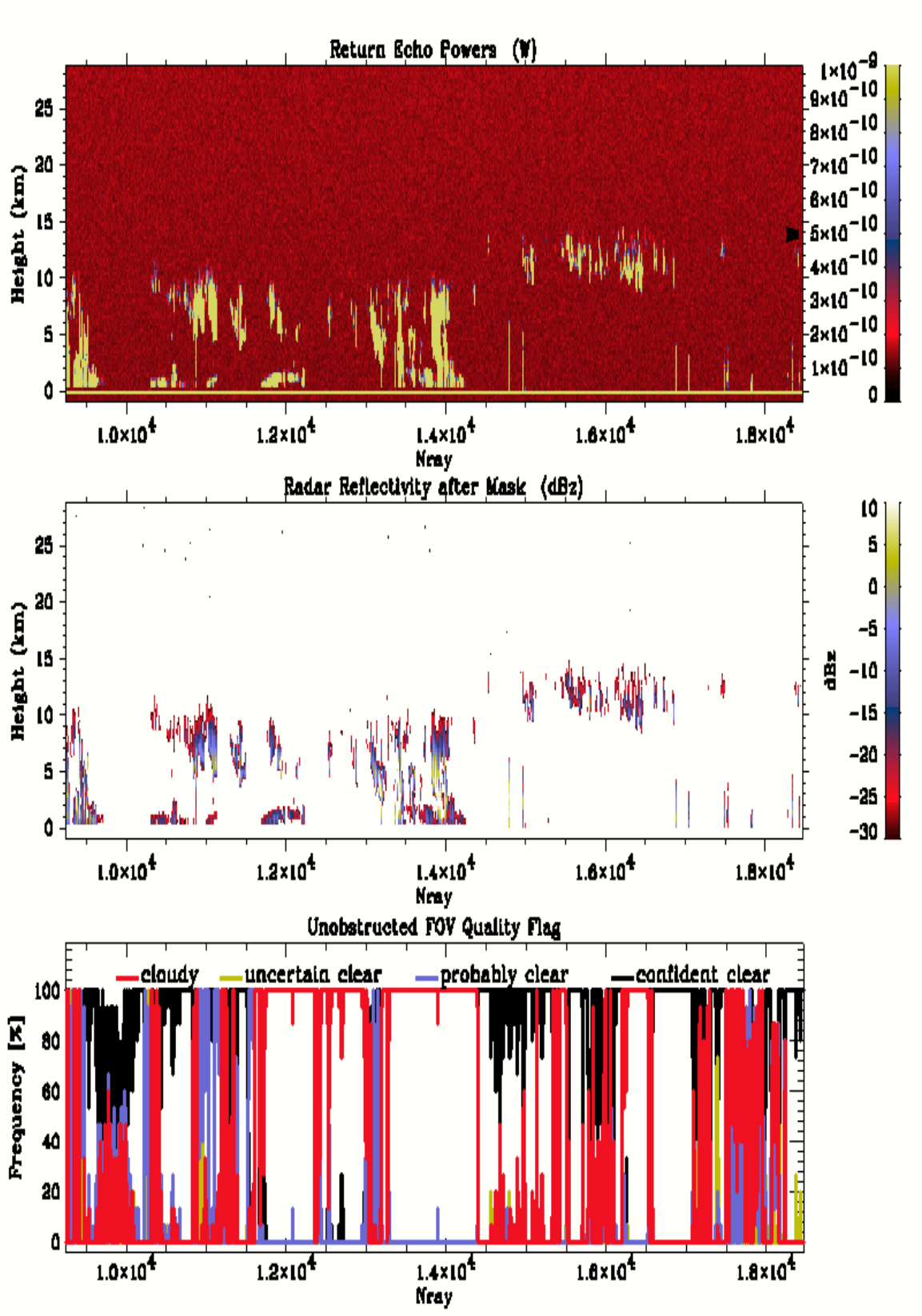

Figure 3(b). Return echo power before significant echo mask and radar reflectivity after mask (section 2).

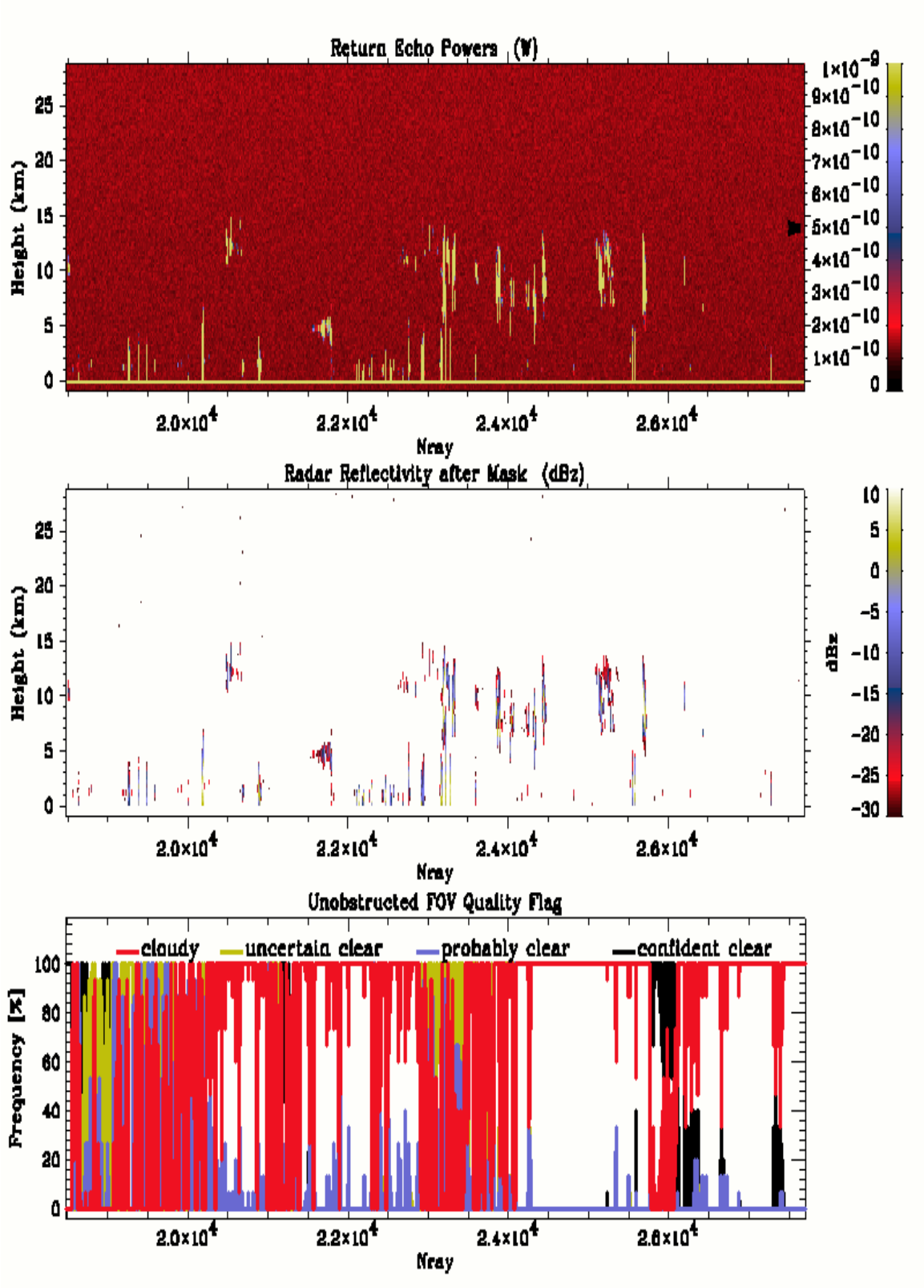

Figure 3(c). Return echo power before significant echo mask and radar reflectivity after mask (section 3).

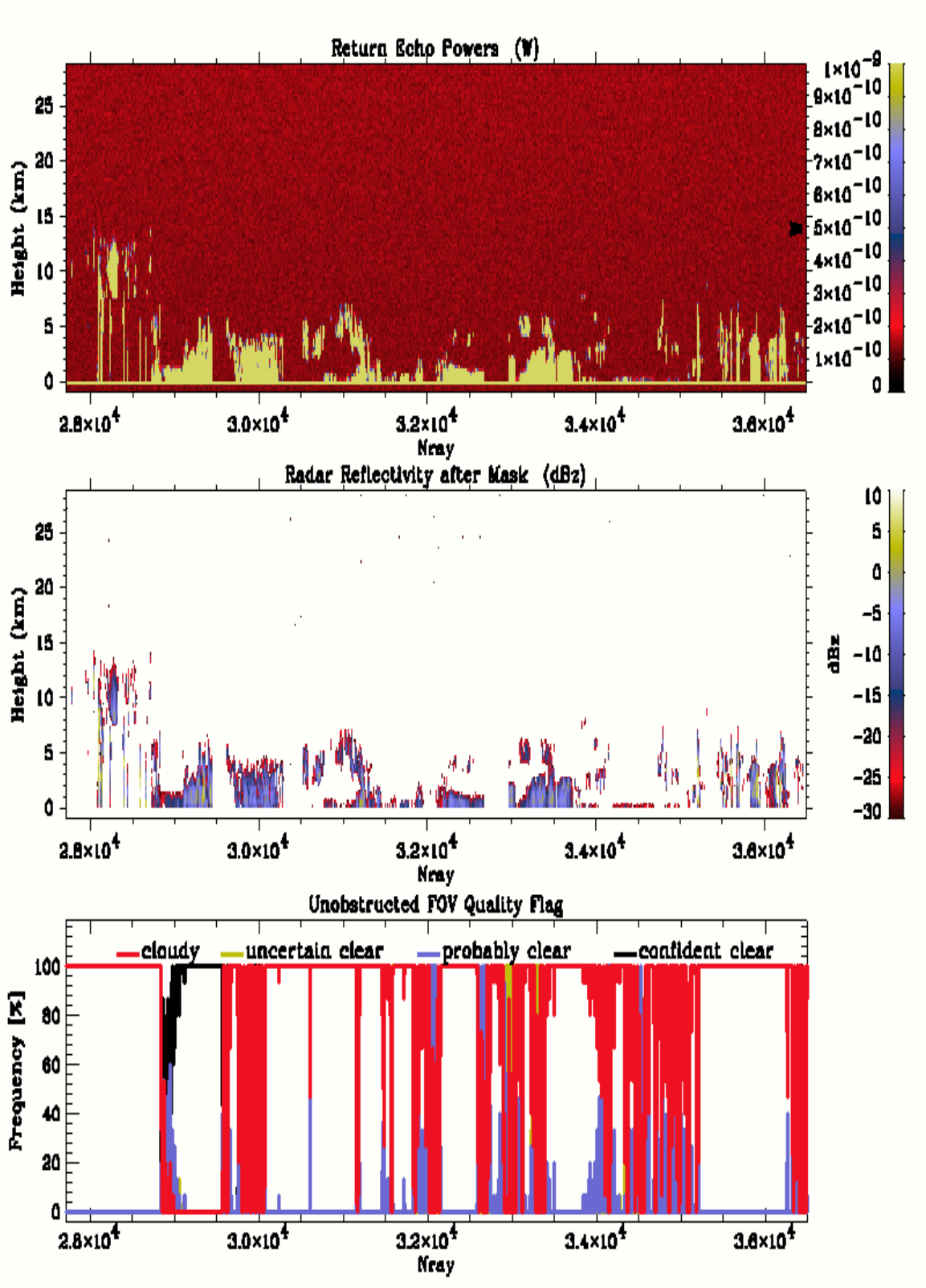

Figure 3(d). Return echo power before significant echo mask and radar reflectivity after mask (section 4).

B2. Diagnostic statistics ASCII output

Description of the ASCII file:

1. The first block of the ASCII output shows diagnostic statistics results of the CLOUDSAT profiles. It shows how many CloudSat rays (nray) and bins (nbin) were found in one orbit, which rays and bins are included in the diagnostic statistic analyses, and the number of cloudy profiles and how many profiles were found without cloud.

2. The second block shows the statistics of the MODIS 48 cloud mask bits.

   The first column is the number of the bytes for saving cloud mask information. The second column is the number of bits in each byte. There are 6 bytes for saving MODIS cloud mask information. Each byte has 8 bits. There are totally 48 bits are used for saving MODIS mask information. The third column shows the number of total bits.

   The fourth column shows the number pixels where bits are equal to zero. The fifth column shows the number of pixels where bits are equal to 1. Column 6 to 9 are used for bits 1-2 and bits 6-7.

3. Block 3 is for the frequency of occurrence of MODIS Cloud Classification. The first column is the type of MODIS Cloud Classification. The second column is the numerical designation Classification (see Table 3 for the definition). Column 3 to 10 are the frequency of MODIS Cloud Classification in eight different regions. The orbit is divided into following seven sections.

Orbit	– the whole orbit	
Tropic	– tropic	(23.5 S to 23.5 N)
N_Sub_Tropic	– north subtropics	(23.5 N - 35 N)
S_Sub_Tropic	– south subtropics	(23.5 S - 35 S)
N_Mid_Lat	– north middle latitude	(35 N - 55 N)
S_Mid_Lat	– south middle latitude	(35 S - 55 S)
N_High_Lat	– north high latitude	(55 N - 90 N)
S_High_Lat	– south high latitude	(55 S - 90 S)

4. Block 4 shows the statistics of CPR Echo Top Cloud Classification. The first column is the type of CPR Echo Top Cloud Classification. The second column is the numerical designation classification (see Table 4 for the definition). Column 3 to 10 are the number of CPR Echo Top Cloud Classifications in the eight different regions.

5. Block 5 shows the statistics of the MODIS CloudSat Scene Variability. The first and second columns are the type of MODIS CloudSat Scene Variability (see

Table 5 for the definition). Column 3 to 10 are the statistic number of MODIS CloudSat Scene Variability in eight different regions. Same as above, the orbit is divided into following seven sections for statistics.

The following is a sample of the diagnostic statistics ASCII output.

```
============================================================
================    Statistic of CloudSat Profiles   =========
============================================================

nray (Profiles) =        36495
           nbin =          125

Profiles:    from            1 to        36495
Height:      from            1 to          125

Total profiles with cloud    :        18962
Total profiles without cloud :        17533

================================================================================
=================          MODIS cloud mask statistic        =================
 Bit         0         1          00         01        10        11
================================================================================
  0       1206    546219
  1     343221    204204       311011     32210     56968    147236
  2     367979    179446
  3     266189    281236
  4     104268    443157
  5     113253    434172
  6     353019    194406       342978     10041     22276    172130
  7     365254    182171
  8      16193    531232
  9       1772    545653
 10       1510    545915
 11       7818    539607
 12       1369    546056
 13     117225    179484
 14     204170    343255
 15       3080    544345
 16      70227    211009
 17      26543    117116
 18     147425    286747
 19     202949    344476
 20     188585     77635
 21     138674    127487
 22       3162    271364
 23          0    272930
 24       1310    304114
 25     268255     28454
 26     541746      5679
 27     522368     25057
 28       1383    546042
 29       1376    546049
 30       1369    546056
 31       1369    546056
 32     503181     44244
 33     503294     44131
 34     503223     44202
 35     503194     44231
 36     503218     44207
 37     503087     44338
 38     503012     44413
 39     503147     44278
 40     503011     44414
 41     503152     44273
 42     503012     44413
 43     502863     44562
 44     502998     44427
```

45	503063	44362
46	502960	44465
47	502971	44454

SUM of MODIS Cloud Classification

		Whole Orbit	Tropic	N_Sub_ Tropic	S_Sub_ Tropic	N_Mid _Lat	S_Mid _Lat	N_High _Lat	S_High _Lat
Unclassifiable	(9)	4644	1975	24	1107	426	987	51	74
No Test	(0)	83	58	25	0	0	0	0	0
Clear	(1)	13596	3561	1757	299	2035	558	4144	1242
High Cloud	(2)	3757	244	298	0	325	0	1052	1838
High Cloud Very Thin	(3)	178	37	0	0	64	0	77	0
High Cloud Thin	(4)	73	60	2	0	0	0	0	11
High Cloud Think	(5)	3835	138	47	1	52	0	771	2826
Non High Cloud	(6)	8940	3464	201	893	886	2158	583	755
Mid Cloud Thick	(7)	1389	40	0	59	351	448	266	225
Low Cloud	(8)	0	0	0	0	0	0	0	0

SUM of CPR Echo Top Cloud Classification

		Whole Orbit	Tropic	N_Sub_ Tropic	S_Sub_ Tropic	N-Mid _Lat	S_Mid _Lat	N_High _Lat	S_High _Lat
No Determination	(0)	0	0	0	0	0	0	0	0
Clear Profile	(1)	17533	4939	1202	839	2002	1932	2952	3667
High Cloud	(2)	9916	2676	1057	672	667	1380	1050	2414
Mid Level Cloud	(3)	3630	52	37	216	600	81	2092	552
Low Level Cloud	(4)	2174	1402	27	217	329	168	0	31
Multi Layer	(5)	3242	508	31	415	541	590	850	307

SUM of Scence Variability

		Whole Orbit	Tropic	N_Sub_ Tropic	S_Sub_ Tropic	N_Mid _Lat	S_Mid _Lat	N_High _Lat	S_High _Lat
No Determination		0	0	0	0	0	0	0	0
Highly Uniform	>= 0.9	21367	4210	1545	699	2895	1578	5177	5263
Uniform	>= 0.75	4049	1117	334	187	379	487	767	778
Low Uniform	>= 0.5	5989	2133	411	308	436	986	890	825
Variable	< 0.5	1473	621	40	92	224	338	96	62
Highly Variable	=< 0.25	3617	1496	24	1073	205	762	14	43

B3. Plots of the diagnostic statistics for quality assessment purposes

The following gives a sample of the diagnostic statistics plots for the quality assessment purposes.

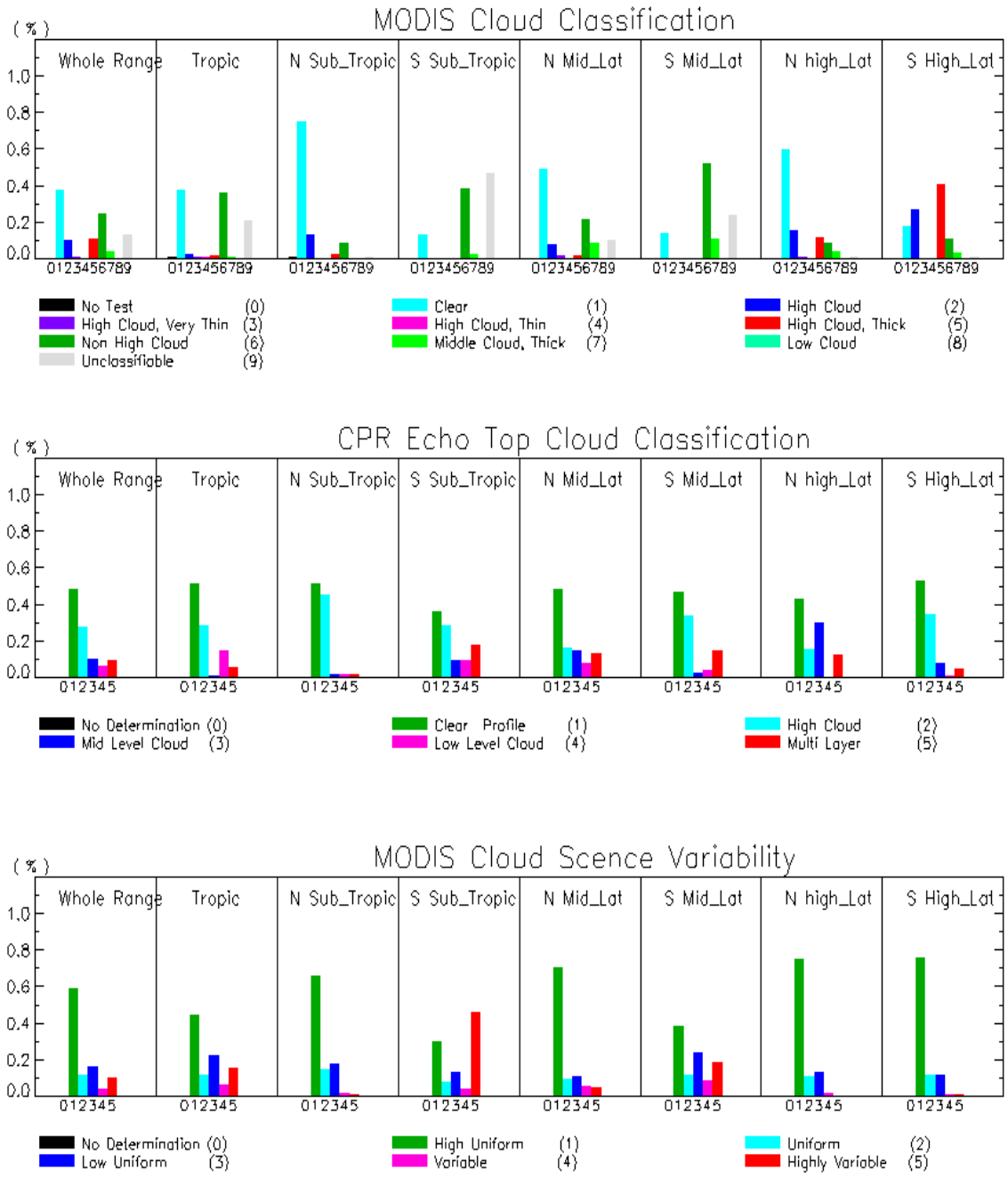

Figure 4. The diagnostic statistics plots. The upper panel is the MODIS cloud classification (block 3 in the diagnostic statistics ASCII output). The middle panel is CloudSat CPR echo top cloud classification (block 4 in the ASCII output). The lower panel is MODIS CloudSat scene variability (block 5 in the ASCII output).

Appendix C. Validation Data Set

193 TERRA cases

29 TERRA TWPC2 Day Cases

Case Number	Date	Julian Day	Time(UTC)	Viewing Angle
1	20000901	245	23:48:30	28.5
2	20000905	249	23:24:07	27.9
3	20000912	256	23:30:01	14.6
4	20000919	263	23:35:56	0.3
5	20000926	270	23:41:44	14.5
6	20010718	199	23:41:30	27.6
7	20010720	201	23:29:15	1.7
8	20010722	203	23:17:07	28.7
9	20010803	215	23:41:22	28.1
10	20010805	217	23:29:06	0.4
11	20010812	224	23:35:02	14.9
12	20010814	226	23:22:46	14.9
13	20010819	231	23:40:57	28.2
14	20010821	233	23:28:41	0.9
15	20010906	249	23:27:53	1.1
16	20010913	256	23:33:32	13.4
17	20010920	263	23:39:31	25.7
18	20011102	306	23:19:46	16.5
19	20011111	315	23:13:24	29.6
20	20011116	320	23:31:25	13
21	20011118	322	23:19:23	17
22	20011123	327	23:37:41	27.4
23	20011125	329	23:25:25	1
24	20011202	336	23:31:20	14.1
25	20011213	347	23:12:26	29.5
26	20011218	352	23:30:13	12.7
27	20011220	354	23:17:42	17.6
28	20011225	359	23:36:30	27.1
29	20011227	361	23:24:15	2

28 TERRA TWPC2 Night Cases

Case Number	Date	Julian Day	Time(UTC)	Viewing Angle
30	20000901	245	11:26:54	23.3
31	20000906	250	11:45:13	20.4
32	20000908	252	11:32:58	9.1
33	20000924	268	11:32:33	9.7
34	20010709	190	11:26:07	11.1
35	20010718	199	11:19:55	24.3
36	20010723	204	11:38:14	19.6
37	20010803	215	11;19:47	23.7
38	20010810	222	11:25:42	9.8
39	20010819	231	11:19:23	23.6

40	20010902	245	11:30:58	5.2
41	20010909	252	11:36:37	19.2
42	20010911	254	11:24:22	10.7
43	20010918	261	11:29:54	3.4
44	20010921	263	11:17:31	25.7
45	20010925	268	11:36:15	19.1
46	20011029	302	11:22:46	11.4
47	20011105	309	11:28:44	3.9
48	20011112	316	11:34:31	18.5
49	20011114	318	11:22:16	11.4
50	20011121	325	11:27:48	3.2
51	20011128	332	11:34:16	19.3
52	20011130	334	11:22:01	10.6
53	20011214	348	11:33:27	18.5
54	20011216	350	11:21:04	11.4
55	20011223	357	11:27:10	4.3
56	20011225	359	11:14:55	24.8
57	20011230	364	11:33:13	18.9

36 TERRA SGP day cases

Case number	Date	Julian Day	Time(UTC)	Viewing Angle
58	20000911	255	17:39:48	2.9
59	20001011	285	17:51:00	24.5
60	20001020	294	17:44:48	13.6
61	20001107	312	17:32:10	10.7
62	20001127	332	17:07:14	47.8
63	20001128	333	17:49:55	24.1
64	20001130	335	17:37:39	1
65	20001205	340	17:55:33	33
66	20001207	342	17:43:23	12.4
67	20001220	355	17:13:04	40.5
68	20001223	358	17:43:38	13.5
69	20010108	8	17:43:12	13.3
70	20010115	15	17:48:59	23.8
71	20010124	24	17:42:59	13.4
72	20010209	40	17:42:57	13.9
73	20010211	42	17:30:42	10.1
74	20010218	49	17:36:37	2
75	20010225	56	17:42:25	13.7
76	20010227	58	17:30:09	10.4
77	20010306	65	17:35:57	1.3
78	20010308	67	17:23:33	22.2
79	20010322	81	17:35:27	2.1
80	20010329	88	17:41:30	13.3
81	20010403	93	17:59:31	41.6
82	20010409	99	17:22:49	22.1
83	20010416	106	17:28:57	10.7
84	20010420	110	17:04:29	47.4

85	20010516	136	17:40:35	13.8
86	20010518	138	17:28:20	10.4
87	20010527	147	17:22:08	21.4
88	20010606	157	17:58:21	42.2
89	20010822	234	17:26:12	9.6
90	20010905	248	17:37:39	14
91	20010907	250	17:25:24	10.1
92	20010916	259	17:18:51	22.2
93	20010923	266	17:24:46	10.4

27 TERRA SGP night cases

Case number	Date	Julian Day	Time(UTC)	Viewing Angle
94	20000820	233	4:36:51	24.4
95	20000919	263	4:48:50	2.1
96	20001007	281	4:35:55	25.1
97	20001021	295	4:47:54	2.3
98	20001108	313	4:35:16	25.2
99	20001115	320	4:41:19	14.3
100	20001122	327	4:47:15	3.1
101	20010107	7	4:58:43	20.9
102	20010116	16	4:52:07	8.9
103	20010123	23	4:58:20	20.7
104	20010127	27	4:33:57	25.2
105	20010203	34	4:40:00	14.2
106	20010208	39	4:58:19	21.3
107	20010217	48	4:51:59	9.9
108	20010224	55	4:57:55	21.1
109	20010226	57	4:45:40	3.1
110	20010323	82	4:38:41	14.8
111	20010330	89	4:44:37	3.7
112	20010408	98	4:38:18	14.9
113	20010510	130	4:37:38	14.5
114	20010609	160	4:47:41	7
115	20010711	192	4:48:18	9.5
116	20010906	249	4:40:47	3
117	20010913	256	4:46:27	9.4
118	20010915	258	4:34:12	14.9
119	20010922	265	4:40:16	2.9
120	20010924	267	4:28:01	25.2

27 TERRA NSA day cases

Case Number	Date	Julian Day	Time(UTC)	Viewing Angle
121	20000304	64	23:09:23	13.6
122	20000306	66	22:57:15	5.3
123	20000312	72	22:20:28	20.7
124	20000326	86	22:33:34	11.8

125	20000407	98	22:58:09	5.8
126	20000416	107	22:52:10	1.9
127	20000427	118	22:34:12	11.6
128	20000506	127	22:27:40	15.7
129	20000710	192	23:09:53	14.5
130	20000923	267	22:50:52	2.1
131	20001009	283	22:50:15	2
132	20001018	292	22:44:02	2.5
133	20001130	335	22:24:38	16
134	20001219	354	22:55:09	6.3
135	20001223	358	22:30:37	11.3
136	20001224	359	23:13:26	18.3
137	20001228	363	22:48:55	2.4
138	20010101	1	22:24:19	15.6
139	20010107	7	23:25:16	25.3
140	20010110	10	22:17:48	20.1
141	20010115	15	22:35:58	7.2
142	20010118	18	23:06:21	14.2
143	20010205	36	22:54:28	6.6
144	20010209	40	22:29:57	11.3
145	20010315	74	23:53:57	39.3
146	20010317	76	22:04:10	27.8
147	20010320	79	22:34:43	7

46 TERRA NSA Night cases

Case Number	Date	Julian Day	Time(UTC)	Viewing Angle
148	20000304	64	8:09:58	28.8
149	20000305	65	7:14:50	9.2
150	20000319	79	7:27:30	1.8
151	20000325	85	6:51:16	24.1
152	20000326	86	7:34:05	4.5
153	20000328	88	7:21:50	4.6
154	20000406	97	7:15:53	8.8
155	20000420	111	7:28:17	0.3
156	20000524	145	7:15:30	9.6
157	20000801	214	7:32:44	3.6
158	20000902	246	7:33:33	4
159	20000904	248	7:21:17	4.7
160	20000918	262	7:33:16	4
161	20000920	264	7:21:01	5.3
162	20001009	283	7:50:48	16.6
163	20001013	287	7:26:18	1.4
164	20001015	289	7:14:02	9.5
165	20001020	294	7:32:21	3.8
166	20001029	303	7:25:53	2.1
167	20001105	310	7:31:50	3.4
168	20001107	312	7:19:35	5.5
169	20001125	330	7:07:03	13.7

170	20001130	335	7:25:13	2.2
171	20001204	339	7:00:27	17.8
172	20001216	351	7:24:59	1.3
173	20001217	352	8:07:56	28.5
174	20001221	356	7:43:26	12.2
175	20001223	358	7:31:10	3.4
176	20001227	362	7:06:39	13.6
177	20001228	363	7:49:29	16.6
178	20010101	1	7:24:54	1
179	20010110	10	7:18:31	5.9
180	20010113	13	7:48:52	16.4
181	20010115	15	7:36:33	7.6
182	20010119	19	7:11:59	9.8
183	20010128	28	7:06:00	13.7
184	20010131	31	7:36:35	7.9
185	20010206	37	6:59:56	17.5
186	20010209	40	7:30:23	4.1
187	20010211	42	7:18:07	5.6
188	20010215	46	6:53:37	21.2
189	20010217	48	6:41:21	27.9
190	20010316	75	6:21:51	36.8
191	20010316	75	7:59:37	24.3
192	20010318	77	7:47:30	16.1
193	20010320	79	7:35:16	7.5

110 AQUA cases

11 AQUA TWPC2 day cases

Case Number	Date	Julian Day	Time(UTC)	Viewing Angle
194	20030920	263	2:20:28	10.6
195	20030927	270	2:26:31	4.3
196	20031013	286	2:26:24	4.5
197	20031020	293	2:32:35	18.8
198	20031022	295	2:20:28	10.9
199	20031024	297	2:08:13	36.5
200	20031029	302	2:26:31	4.4
201	20031031	304	2:14:16	24.9
202	20031105	309	2:32:19	18.1
203	20031116	320	2:14:32	24.3
204	20031121	325	2:32:59	19.7

18 AQUA TWPC2 night cases

Case Number	Date	Julian Day	Time(UTC)	Viewing Angle
205	20030917	260	14:11:29	29.1
206	20030922	265	14:29:48	13.8
207	20030924	267	14:17:32	16.1

208	20031001	274	14:23:36	1.8
209	20031008	281	14:29:31	13.2
210	20031010	283	14:17:25	16.5
211	20031017	290	14:23:37	2.5
212	20031022	295	14:41:55	38.4
213	20031026	299	14:17;32	16.2
214	20031031	304	14:35:42	27
215	20031102	306	14:23:26	2
216	20031109	313	14:29:43	13.5
217	20031111	315	14:17:35	16.1
218	20031116	320	14:36:01	27.6
219	20031118	322	14:24:02	2.3
220	20031120	324	14:11:54	28.6
221	20031123	327	14:42:28	39.2
222	20031125	329	14:30:12	14.9

22 AQUA SGP day cases

Case Number	Date	Julian Day	Time(UTC)	Viewing Angle
223	20020821	233	19:19:22	35.4
224	20020824	236	19:49:53	19.9
225	20020911	254	19:37:34	3.9
226	20020913	256	19:25:10	26
227	20020916	259	19:55:28	30.1
228	20020920	263	19:31:19	15
229	20021002	275	19:56:04	31.3
230	20021004	277	19:43:56	10.1
231	20021008	281	19:19:24	34.3
232	20021011	284	19:45:50	21.1
233	20021013	286	19:37:34	2.9
234	20021018	291	19:55:28	30.8
235	20021020	293	19:43:25	9.5
236	20021022	295	19:31:19	14.3
237	20021024	297	19:19:10	34.5
238	20021027	300	19:49:35	21.1
239	20021031	304	19:25:04	25.2
240	20021105	309	19:43:14	9.4
241	20021119	323	19:55:18	30.9
242	20021216	350	19:36:50	2.5
243	20021223	357	19:43:00	9.7
244	20021230	364	19:48:54	20.8

10 AQUA SGP night cases

Case Number	Date	Julian Day	Time(UTC)	Viewing Angle
245	20020830	242	8:10:11	32.5
246	20020904	247	8:28:29	1.4
247	20020912	255	9:16:50	62.6

248	20020913	256	8:22:01	11.7
249	20020922	265	8:15:59	22.5
250	20021008	281	8:16:14	21.7
251	20021013	286	8:34:24	13.4
252	20021020	293	8:40:13	24.1
253	20021029	302	8:34:09	13.5
254	20021109	313	8:15:25	22.5

9 AQUA NSA night cases

Case Number	Date	Julian Day	Time(UTC)	Viewing Angle
272	20020905	248	13:58:10	14.2
273	20020909	252	13:33:39	3
274	20020914	257	13:51:49	10
275	20020916	259	13:39:25	1.4
276	20020927	270	13:21:33	11.6
277	20021018	291	13:39:25	2
278	20021029	302	13:21:08	11.6
279	20021030	303	14:03:57	18.1
280	20021105	309	13:27:03	7.2

23 AQUA NSA snow night cases

Case Number	Date	Julian Day	Time(UTC)	Viewing Angle
281	20020902	245	13:27:36	7.6
282	20021023	296	13:57:56	14.3
283	20021024	297	13:02:50	24.1
284	20021025	298	13:45:39	6.3
285	20021110	314	13;45:05	5.7
286	20021114	318	13:20:31	11.8
287	20021117	321	13:51:13	10.1
288	20021124	328	22:03:05	9.6
289	20021125	329	22:45:55	20.8
290	20021129	333	22:21:24	3.6
291	20021204	338	22:39:42	16.6
292	20021206	340	22:27:26	7.9
293	20021209	343	13:14:32	15.9
294	20021213	347	22:33:12	12.3
295	20021216	350	13:20:38	11.6
296	20021225	359	13:14:33	15.8
297	20030101	1	13:20:28	11.7
298	20030104	4	21:56:27	13.8
299	20030106	6	13:38:49	1.7
300	20030109	9	22:14:57	1.1
301	20030114	14	22:33:23	12.5
302	20030115	15	13:32:45	3.4
303	20030116	16	22:21:08	3.9